

## Characterization of nanoparticle systems by Mössbauer and positron annihilation spectroscopic methods

Sanjukta Ghosh\*, M Chakrabarti and D Banerjee<sup>†</sup>

DSA Laboratory, Department of Physics, University of Calcutta,  
92, A. P. C. Road, Kolkata-700 009, India

**Abstract** : Mössbauer spectroscopy (MS) and positron annihilation lifetime spectroscopy (PALS) are two very useful technique for determining the magnetic properties and defects in the materials respectively. These properties of nanocomposites are quite different from those of bulk solids. Thus the Mössbauer parameters namely isomer shift, quadrupole splitting and hyperfine field are very useful to understand the magnetic properties of the nanoparticle systems. The lifetime of positrons and the defects in the lattice sites are greatly influenced by the size of grain boundaries. Hence PALS is also a sensitive non-destructive tool to understand the nanoparticle systems. These two techniques are discussed in this paper.

**Keywords** : Nanoparticles, ferrites, semiconductor, Mössbauer spectroscopy, positron annihilation lifetime spectroscopy.

**PACS Nos.** : 75.50 Gg, 81.07.-b, 76.80.+y, 78.70.Bj

### 1. Introduction

“Nanomaterials” is the keyword of the forthcoming technology. Sine last few couple of years some of these nanoparticles are widely investigated. Not only in the field of physics but also in chemistry, biological science and other application oriented field the nanoparticles have started to dominate over microparticles due to their fundamental characteristics. Specially the magnetic materials like ferrites are showing some unusual behaviour as an effect of nanoscale confinement. Other materials like semiconductors, metals, amorphous materials, superconductors, layered structures are showing new exciting properties when their grain diameters are decreased to nanometer range. Basically the term “nanoparticle” gives upper and lower limit of grain size and it is 1-100 nm. Within this particular range of size the basic fundamental characteristics of the materials strongly differ from that of the bulk. Some scientists, to get a relevant answer of the unusual behaviour of nanoparticles, have suggested various theoretical concepts or models. In most of the cases the logic is yet to explore. Thus it has become a challenge to the modern technology to engineer the nanoscale materials for better applications. We are mainly dealing with magnetic materials like ferrites and iron oxide in nano order range. It is not unknown that ferrites are magnetic materials combining insulating and ferromagnetic properties and they have versatile application in

the field of information technology, microwave devices and magnetic storage media. Nanoparticles are very dependent on the way of their preparation or synthesis. Even the preparation technique can also tune the magnetic, electrical, surface and mechanical properties of the nanoparticles. Some of the famous or common processes are high-energy mechanical milling, r.f. sputtering, sol-gel technique, chemical vapour deposition, physical vapour deposition, ion beam sputtering and other methods. Presently we will be discussing about the mechanical milling method though some work on sputtering technique have been presented in the other paper. Main emphasis we are giving on the ferric oxide ( $\text{Fe}_2\text{O}_3$ ), chromium and indium doped magnesium ferrites ( $\text{Mg}_{1.0}\text{Fe}_{1.5}\text{Cr}_{0.5}\text{O}_4$ ,  $\text{Mg}_{1.0}\text{Mn}_{0.1}\text{Fe}_{(1.9-x)}\text{In}_x\text{O}_4$ ). Some extensive studies have been done on many ferrite nanoparticles like nickel ferrite, zinc ferrite, manganese ferrites, garnets *etc.* Mostly in all the cases it is observed the basic magnetic nature changes. The parameters like saturation magnetization, curie temperature, coercivity *etc.* all shows a very strong deflection from the conventional values. Formation of some new phases has also been observed. We mainly study the magnetic effects from variations of the parameters of Mössbauer Spectroscopy technique. In ferrites the effect of two sites namely tetrahedral (A) and octahedral (B) sites can be explained by the above technique. Thus the effect of s-electron density, nuclear charge distribution and internal magnetic field can be explained from the point of view of nanoparticles. We will also discuss

<sup>†</sup> Deceased

\* Corresponding Author

about the super paramagnetism in ferrites. We will emphasize on the grain boundary effects, surface effects and volume effects of nanoparticles observed from the parameters of Mössbauer Spectroscopy. We will also discuss about nanoparticles of copper oxide. In high  $T_c$  superconductors the CuO plane is superconducting though CuO itself is a semiconductor with narrow band gap. Thus we are also studying CuO with the help of Positron Annihilation Lifetime Spectroscopy.

Mössbauer Spectroscopy (MS) is a well-known nuclear technique in the field of material physics in determining various magnetic properties of materials like ferrites, Fe alloys and other iron compounds [1-4].  $^{57}\text{Fe}$  is a very sensitive and popular Mössbauer nucleus using 14.4 KeV  $\gamma$ -transition. The parent nucleus used here is  $^{57}\text{Co}$  (half life = 270 days). The parent nucleus decays by the capture of electron to 136.32 KeV level of  $^{57}\text{Fe}$  with high efficiency. From this level 91% of the decays approach to the 14.41 KeV level which is the level of interest for Mössbauer resonance. We give importance to three main parameters namely isomer shift (IS), quadrupole splitting (QS) and hyperfine field (HF). The isomer shift is a measure of the difference of electron density at the nuclear site between the absorbing and emitting nuclei. The origin of isomer shift lies in the fact that an atomic nucleus has a finite volume and  $s$ -electrons have a finite probability of penetrating the nucleus and spending a fraction of their time inside the nucleus and spending a fraction of their time outside the nucleus. Due to Coulomb interaction of the nuclear charge distribution with the  $s$ -electron charge cloud inside the nuclear dimension, the ground and the excited energy levels get shifted by a very small amount  $\delta E$ , which is equal to the energy difference of the electrostatic interaction of a point nucleus and a nucleus with finite radius. Since the size of the nucleus differs in its ground state and excited state, the  $\delta E$  varies in each nuclear state. Therefore in nuclear transition, due to this volume effect, the energy of the gamma ray will change. The electron densities of the resonating nuclei in the source (S) and absorber (A) may differ due to their differences in chemical and physical environments. Thus the isomer shift will be the difference in electrostatic shift between the source and the absorber. An external Doppler velocity is applied in the Mössbauer experiment to bring a resonance between the emitted energy and absorption energy. So the isomer shift is mainly dependent on the  $s$ -electron densities. The variation in  $s$ -electron densities arise generally due to two reasons : (a) alteration of  $s$ -electron population in the valence shell, (b) shielding of  $s$ -electrons by the electrons of  $p$ -,  $d$ - and  $f$ -orbital. Thus, isomer shift gives very useful information on electron configuration, spin and oxidation state of a Mössbauer atom. Initially when we discuss about isomer shift based on the electric monopole interaction, we assume the nucleus to be spherically symmetrical and the nuclear charge to be uniformly distributed. But as a matter of fact in most of the nuclei the nuclear charge distribution is not uniform and spherically

symmetrical. This asymmetry gives rise to the electric quadrupole interaction and consequently we observe quadrupole splitting in the Mössbauer spectra. Electric quadrupole splitting arises from the interaction of electric quadrupole moment with an inhomogeneous electric field described by electric field gradient (EFG) contribution. The nuclear quadrupole moment measures the deviation of the nuclear shape from spherical configuration. This deviation may differ in each state of excitation. The shape of the distorted nucleus is reflected in its sign, which can be positive, or negative determined by whether the nucleus is elongated (prolate) or flattened (oblate). For a Mössbauer nuclide, the quadrupole moment is constant so only EFG can vary. EFG is mainly altered due to physical and chemical influences in the matter. Quadrupole splitting thus plays a very important role in the variation in particle size. The last important parameter we are dealing with is the internal hyperfine field. Hyperfine field results from the contribution of three separate fields and can be written as

$$H_N = H_F + H_D + H_I.$$

$H_I$  is the contribution from orbital magnetic moment of electron ( $-2\beta < 1/r^3 > < L >$ ) where  $\beta$  is Bohr magneton and the expectation values are taken over spatial coordinates and angular momentum of electrons in partly filled shells.  $< L >$  becomes zero in  $s$ -state ions and the case where the orbital momentum is quenched by the electrostatic field of the ligands.  $H_D$  comes from the dipole interaction with the moment of the electron spin ( $-2\beta < \{3r(S.r)/r_5\} - \{S/r^3\} >$ ), here  $H_D$  vanishes for a cubic symmetry. The largest contribution to the internal field arises due to Fermi contact interaction ( $-16\pi/3\{\beta \sum S_i \delta(r_i)\}$ ). The  $\delta$  function implies that only the  $s$ -electrons with finite probability at the nucleus, give rise to the contribution to the sum over all the electron spins. In case of the atom containing a partially filled magnetic shell, there appears a difference in spin up and spin down charge densities even in the filled  $s$ -shells. The exchange interaction between the spin up polarized  $d$  shell and the spin up  $s$ -electron is attractive in nature whereas that between the  $d$ -shell and a spin down  $s$ -electron is repulsive. Consequently the radial parts of the wave functions of two  $s$ -electrons differ. One is pushed towards the nucleus and the other is pulled outward. The spin densities no longer cancel out and thus  $H_F$  occurs. In addition to the above hyperfine field the nucleus of a particular atom sees a local magnetic field due to the presence of magnetic atoms. So basically all these three parameters are expected to show some relevant information regarding the nano regime. The variation in the values of all these parameters in the nano dimension mainly occurs due to the fundamental properties of nanoferrites like grain boundaries, small volume *etc.* So, our aim is to correlate the Mössbauer parameters with the nanoparticle properties. In some cases, the agreement has been done with TEM analysis also. From the hyperfine field, we are even able to calculate the saturation

magnetization and in few cases we observe the nature of the samples in nano range. Grain growth being a main factor in nanoparticles so special emphasis is given on the application of Marshall's equation.

Positron annihilation lifetime spectroscopy technique (PALS) is a well-known non-destructive technique to study the defects in solids [5-8]. Positrons from the radioactive source  $\text{Na}^{22}$  while entering a solid thermalize within 1 to 10 ps by producing electron-hole pairs and phonons. A thermalized positron is in a Bloch like state and its intensity becomes highest in the interstitial regions of lattice. Positrons get highly localized when these are trapped in the lattice defects like vacancies and dislocations. These positrons annihilate with the electrons in the solid in a two-gamma annihilation process, in which two 511 KeV  $\gamma$ -quanta are emitted in opposite directions. Measuring the time of emission, it becomes possible to get useful information about the material. PALS is not restricted like iron compounds in MS but mostly all materials can be used to get the relevant information about the defect sites and electronic structures. The useful parameters are the lifetime components  $\tau_i$  and the intensities  $I_i$  of the positrons, which determine the various lattice defects. These lifetime components will correspond to individual characteristic lifetime of the components, if the sample is a mixture of non-interacting components. If the sample is single component substance, element or compound, with a characteristic Bloch lifetime, detection of two or more lifetime components indicates the presence of trapping sites or other physical processes like positronium formation. The two state trapping model assumes annihilation from Bloch state and from one types of positron traps. The lifetime for annihilation from the positron trap turns out to be longer of the two lifetime components and denoted by  $\tau_2$ . We define a term called lifetime for annihilation from the Bloch state, called  $\tau_B$  and it is expressed as

$$\tau_B = (I_1 + I_2) / (I_1 / \tau_1 + I_2 / \tau_2).$$

So in a trapping model, both  $\tau_B$  and  $\tau_2$  are physically significant quantities. Following the lifetime spectra, we are able to discuss about the defects in the lattice sites. Some works on nanoparticles are going on through PALS, but we will be discussing only about the copper oxide mentioned above. This technique is yet to explore much about its application in the field of nanoparticles.

Thus, our previous results and ongoing works with the help of these two above-mentioned techniques are showing sufficient and relevant information about nanoparticles.

### . Experimental

The samples are prepared by standard ceramic technique from the AR grade chemicals with 99.99 % purity. All the samples namely  $\text{Fe}_2\text{O}_3$ , Cr and In doped Mg ferrites and CuO are ball-milled for several hours to get nanoparticles. Grain size calculation

has been done by Debye-Scherrer method and TEM analysis. Finally the samples are studied using Mössbauer spectroscopy and Positron lifetime spectroscopy.

### 2.1. Mössbauer spectroscopy unit :

The present investigations have been carried out with a constant acceleration spectrometer. We would like to explain our system in three parts : (a) Mossbauer drive system (Model CMTE 250), (b) Digital function generator, (c) Principle of operation.

#### a) Mössbauer drive system

The driving system consists of the electromagnetic Mössbauer velocity transducer (MVT) and the Mössbauer driving unit (MDU). It delivers a precise motion to the  $\gamma$  ray source during the spectrum measurement. The ideal triangular waveform is obtained from a digital function generator, which is transformed into a parabolic waveform by integration. An ideal double parabolic waveform impressed on the drive coil makes the drive move with constant acceleration. To minimize the deviation of the actual source motion from its ideal value both the driving unit and the transducer together act as feedback system.

The Mössbauer velocity transducer is based on the two mechanically coupled loud speaker systems, one, the drive coil generating the motion, and the other, the pick-up coil, measuring the instantaneous velocity by induction. The polarity of the pick-up coil is chosen such that it is opposite to the reference voltage. A difference amplifier circuit in the driving unit compares the pick-up signal from the transducer with the instantaneous value of the reference-input waveform of the function generator representing the true velocity. The voltage difference (error signal) between the reference and the actual velocity sweep, which proportional to the deviation of transducer motion from the desired velocity, is amplified and then fed into the power amplifier providing a negative feedback thus stabilizing the mechanical motion.

The magnetic field in the gap of the pick-up system is constant, which provides a high linearity of the driving system. The magnetic induction is 0.5 T and sensitivity of the pick-up system is  $\approx 50 \text{ mV/mm/s}$ .

#### (b) Digital function generator

The digital function generator supplies the triangular reference signal to the Mössbauer drive circuit, which in turn provides the waveform for the source motion. The triangle is synthesized digitally. The function generator supplies the synchronous signal, which establishes a linear correspondence with the velocity of the drive.

#### c) Principle of Operation

The digital function generator produces an electrical signal having the desired velocity sweep waveform. The

electromagnetic MVT converts this electrical signal into mechanical motion, following integration. The  $\gamma$ -rays passing through the absorber are detected by xenon filled proportional counter coupled to a standard  $\gamma$ -ray pulse height spectrometry system. An electronically regulated high voltage supply ( $-2100\text{V}$ ) is given to the detector. The detector is connected to an active filter linear pulse amplifier (ORTEC 572) through a preamplifier (ORTEC 142PC) from which the pulses are fed into multi channel analyzer for recording the  $\gamma$ -ray spectrum. In the spectrometer the sorting of counts is performed in the MCS mode. Before each experiment the spectrometer is calibrated by  $25\ \mu\text{m}$  Fe foil.

**Table 1.** Mössbauer parameters for different ball-milled samples of  $\text{Fe}_2\text{O}_3$ .

| Samples ( $\text{Fe}_2\text{O}_3$ ) | Isomer shift (mm/s) | Quadrupole splitting (mm/s) | Hyperfine field (Tesla) |
|-------------------------------------|---------------------|-----------------------------|-------------------------|
| Un-milled (62.26 nm)                | 0.41                | -0.08                       | 51.82                   |
| Ground for 5 hrs (7.7 nm)           |                     |                             |                         |
| Six finger                          | 0.37                | 0.15                        | 49.46                   |
| Doublet                             | 0.38                | 2.33                        |                         |
| Ground for 10 hrs (9.12 nm)         |                     |                             |                         |
| Six finger                          | 0.48                | 0.087                       | 49.13                   |
| Doublet                             | 0.40                | 1.79                        |                         |
| Ground for 15 hrs (10.39 nm)        |                     |                             |                         |
| Six finger                          | 0.37                | 0.27                        | 48.89                   |
| Doublet                             | 0.40                | 1.69                        |                         |

## 2.2. Positron annihilation lifetime spectroscopy unit :

In the positron annihilation lifetime spectrometer the source is sandwiched between the samples. The  $\text{BaF}_2$  scintillators are optically coupled to the photomultiplier tubes (PMT, XP2020Q) with DC200 silicon fluid. Two PMTs are used as start channel and stop channel. To calculate the exact lifetime of the positrons before they annihilate a delay is given in the stop channel circuit. High voltage stabilized power supplies are used for providing the bias to the PMT's. The operating voltage has been set to  $-2100$  volts. To eliminate the effect of time walk, the PMT pulses are processed through constant fraction differential discriminator (CFDD) one in each channel. The pulses from CFDD are connected to TAC (time to amplitude converter), which helps to calibrate the spectrometer and to shift the spectrum to a desired region in the multichannel analyzer. The output pulses from TAC whose amplitudes are proportional to the time gap between emission of the  $1.276\ \text{MeV}$  start  $\gamma$ -ray and the subsequent  $0.511\ \text{MeV}$  annihilation stop  $\gamma$ -ray pulses are recorded in a PC based multichannel analyzer.

## 3. Results and discussion

MS is a very useful tool in determining the magnetic properties of nanoparticle ferrites and  $\text{Fe}_2\text{O}_3$ . Here we will be discussing about two types of observations :

- Superparamagnetism for  $\text{Fe}_2\text{O}_3$  (FO) and  $\text{Mg}_{1.0}\text{Fe}_{1.5}\text{Cr}_{0.5}\text{O}_4$  (MFC) (a magnetic sextet dominated by paramagnetic doublet).
- A variation in Mössbauer parameters for  $\text{Mg}_{1.0}\text{Mn}_{0.1}\text{Fe}_{1.9-x}\text{In}_x\text{O}_4$  ( $x = 0.3, 0.9$ ) (named as M3 and M9 respectively).

Let us first discuss about the observation of superparamagnetism at room temperature of FO and MFC sample as shown in Figures 1 and 2. For FO sample 4 different grinding hours are used. From the XRD line profile the grain size calculation is done. The grain size decreases with the increase in milling hour. The super paramagnetic nature is obtained in each case of grinding. The hyperfine field decreases very slowly with the increasing in milling hours. A similar pattern of spectrum is observed for MFC samples. The grain size of MFC has come out to be  $25\ \text{nm}$  from XRD. At this stage, the volumes of the grains reduce and a transformation takes place from multidomain to single domain structure. At single domain, the spins start flipping along the various easy axes of magnetization. This phenomenon is a special feature of nanoferrites. Physical interpretation can be given from the following Arrhenius law,

$$\tau = \tau_0 \exp(KV/k_B T) \quad (1)$$

$\tau_0$  = relaxation time of MS,  $\tau$  = relaxation time of the spins,  $K$  = anisotropy constant,  $V$  = volume,  $k_B$  = Boltzmann's constant,  $T$  = temperature.

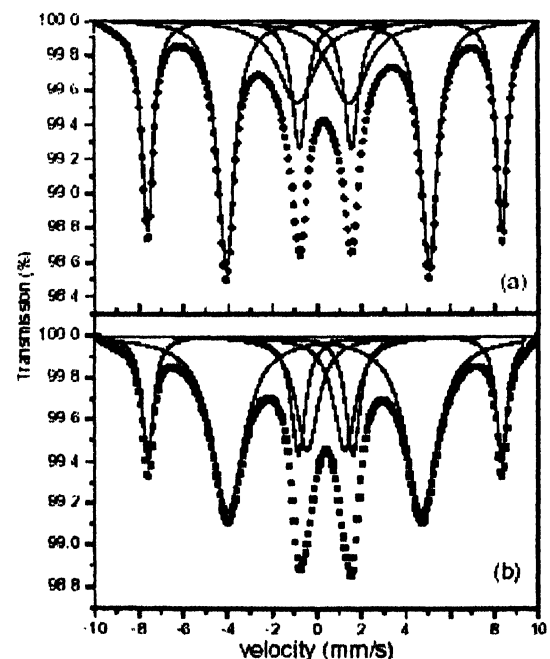


**Figure 1.** The Mössbauer spectra of (a)  $\text{Fe}_2\text{O}_3$  milled for 5 hrs and (b)  $\text{Fe}_2\text{O}_3$  milled for 15 hrs.

For lower grain sizes, as  $V$  becomes less therefore  $KV$  becomes comparable with  $k_B T$  i.e. thermal energy becomes comparable with anisotropy energy. The spins get thermally induced and fluctuates from one potential well to other. Here the easy axes of magnetization act as the potential wells. The

spins possess high magnetic moment so in the spectrum, magnetic sextet is present. But the relaxation time of the spin fluctuations are less than the measuring time of MS and thus the system acts as paramagnetic showing a strong doublet at the center.

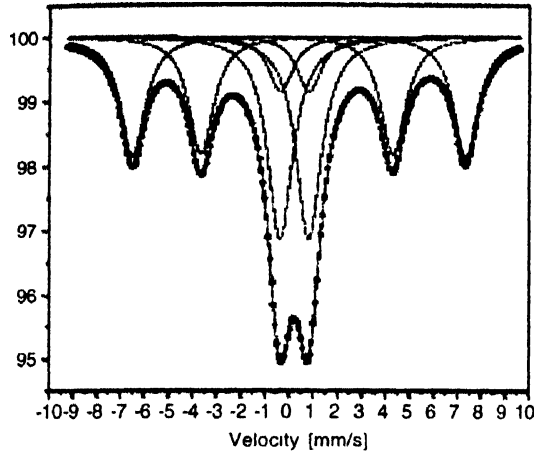


Figure 2. The superparamagnetic spectrum of 36 hrs milled  $Mg_{10}Fe_{15}Cr_{05}O_4$

We next discuss about M3 and M9 samples. The sizes obtained are nearly 36 nm and 25 nm after milling for 22 hrs (M322, M922) and 48 hrs (M348, M948). According to the bulk nature M3 shows magnetic sextet and M9 shows paramagnetic doublet. After reduction in size the spectrum of the samples M322 and M348 show same magnetic sextet and paramagnetic doublet for M922 and M948 samples. But with reduction in grain size the parameters IS, QS and HF varies. From Table 2 in M3 series we observe IS decreases in B site and increases in A site with the reduction in particle size. This represents the *s*-electron density increases in tetrahedral site and decreases in octahedral site. In M9 series we observe a variation in IS value in both the sites with decrease in particle size. This variation in IS in each case may also occur due to shielding of *s*-electrons. As we know that the nuclear charge distributions are not uniform thus

the spherical symmetry is disturbed. In our series due to the above-mentioned reason there is existence of magnetic dipole and electric quadrupole interaction. These give rise to quadrupole splitting. For both M3 and M9 series, we observe QS increases in tetrahedral (A) site and decreases in octahedral (B) site with decrease in particle size. As the electric quadrupole moment is constant for a given Mössbauer nuclide so the observed changes arises from the electric field gradient (EFG) contribution. EFG usually alters by the physical and chemical changes in the systems. In our nanosize samples the physical changes are influencing the EFG. We expect during ball milling a mechanical deformation takes place in the lattice, which consequently raises the non-cubic symmetry. So the alteration of lattice parameter after strong milling can attribute to the QS variation. We can also consider the theory by Sternheimer, which says the electron shell of a Mössbauer atom distorts in the presence of a non-cubic charge distribution in the surrounding crystal lattice. The nature of variation of HF reflects the magnetic nature of the samples. Again from table one we observe for both the sites HF decreases with decrease in grain size in M3. Therefore to correlate the HF with saturation magnetization we follow Marshall's equation [9],

$$H_n = A M_S \quad (2)$$

$H_n$  = the hyperfine field,  $A$  = constant,  $M_S$  = saturation magnetization.

$$M_S = A_V(H_{NF}) \quad (3)$$

So following eq. (3) we observe  $M_S$  increases with decrease in particle size, which is opposite to dead layer theory. Thus we can say the critical size is not obtained here at room temperature as no superparamagnetism has occurred. Figure 3 and Figure 4 are showing the variation in spectrum with decrease in grain size.

In high  $T_C$  superconductors the CuO plane is superconducting though CuO itself is a semiconductor with a

Table 2. The Mössbauer parameters for nanosize particles

| Sample                             | IS (A) | IS (B) | QS (A) | QS (B) | HF (A) | HF (B) |
|------------------------------------|--------|--------|--------|--------|--------|--------|
| $Mg_{10}Mn_{01}Fe_{(19-x)}In_xO_4$ | mm/s   | mm/s   | mm/s   | mm/s   | KOe    | KOe    |
| M3 ( $x = 0.3$ )<br>(Un-milled)    | -0.174 | 0.453  | -0.185 | 0.140  | 398.23 | 406.14 |
| M322<br>(Milled for 22 hrs)        | 0.231  | 0.407  | 0.041  | 0.114  | 378.34 | 412.2  |
| M348<br>(Milled for 48 hrs)        | 0.324  | 0.296  | 0.086  | 0.055  | 365.43 | 415.6  |
| M9 ( $x = 0.9$ )<br>(Un-milled)    | 0.1917 | 0.188  | 0.413  | 0.574  |        |        |
| M922<br>(Milled for 22 hrs)        | 0.386  | 0.224  | 0.552  | 0.504  |        |        |
| M948<br>(Milled for 48 hrs)        | 0.156  | 0.167  | 0.979  | 0.344  |        |        |